Ex. PGS 1046
(EXCERPTED)

3D Seismic Imaging

Biondo L. Biondi

Investigations in Geophysics Series No. 14

Michael R. Cooper, series editor

Gerry Gardner, volume editor

SOCIETY OF EXPLORATION GEOPHYSICISTS

Tulsa, Oklahoma, U.S.A.

ISBN 0-931830-46-X
ISBN 1-56080-137-9

Society of Exploration Geophysicists
P. O. Box 702740
Tulsa, OK 74170-2740

Published 2006
Printed in the United States of America

Library of Congress Cataloging-in-Publication Data
Biondi, Biondo, 1959-
3D seismic imaging / Biondo L. Biondi.
p. cm. -- (Investigations in geophysics ; no. 14)
Includes bibliographical references and index.
ISBN 0-931830-46-X -- ISBN 1-56080-137-9
1. Three-dimensional imaging. 2. Seismic reflection method. I. Title. II. Title: Three dimensional seismic imaging.
QE538.5.B56 2006 2006050641
551.0285'6693--dc22 CIP

Chapter 9

Imaging and Partial Subsurface Illumination

Introduction

In Chapter 8, we analyzed how the spatial sampling rate influences image quality. If data sampling is not sufficiently dense, the seismic image may lose resolution and/or it may be affected by artifacts.

Unfortunately, however, density of spatial sampling is not the only problem encountered with realistic 3D acquisition geometries. An even more common problem is irregularity of the spatial sampling. Often, irregular sampling in space is a product of practical constraints, examples of which include cable feathering in marine acquisition and surface obstacles in land acquisition. In other cases (e.g., with button-patch geometries), irregular sampling geometry might be inherent in the survey design.

The main effect of irregular sampling geometries is either uneven illumination or incomplete illumination of the subsurface. Such partial illumination causes distortions in the image. In milder cases, distortions are limited to the image amplitudes, and they are clearly visible in depth or time slices. Those distortions often are called acquisition footprint. Figure 1 shows an example of acquisition footprints in a migrated depth slice taken from a marine data set. On the right-hand side, horizontal striping is clearly visible, superimposed over the image of a complex turbidite system with crossing channels. The horizontal striping is not linked to geology; it is along the direction of the sailing lines of the recording vessel.

When subsurface illumination is not only uneven but is also incomplete, the phase of the image is distorted, and strong artifacts are created. At the limit, when the acquisition geometry has holes, the data are aliased, at least locally. In such cases, a distinction between the effects of coarse sampling (which we called aliasing in Chapter 8) and the effects of irregular geometries obviously is artificial. However, it helps to analyze such effects separately and to develop independent methods for alleviating the problems.

Either uneven or incomplete illumination can be caused by complexity of the velocity function in the overburden, as well as by irregular acquisition geometries. Imaging under salt edges is an example of an important task that suffers from partial illumination of the reflectors. The problem often is caused by sharp velocity-model variations that prevent the seismic energy either from reaching the reflectors or from propagating back to the surface. Although the immediate causes of partial illumination differ in the two cases — irregular acquisition geometry versus complex overburden — the final manifestation is the same: The wavefield is not sampled sufficiently at depth for migration to image the reflectors without artifacts. The concepts and methods used to address the uneven-illumination problem are similar, regardless of its origin, and consequently I present them in a unified manner.

When illumination is uneven but without gaps, the image can be improved substantially by a simple normalization of the imaging operator or, as it often is called, by an operator equalization. In this chapter, we introduce the basic concepts of operator equalizations, using a simple imaging operator — interpolation followed by partial stacking — as a proxy for more complex imaging operators. In cases when uneven illumination of the reflectors relates mostly to irregular acquisition geometry and the velocity in the overburden is fairly simple, the DMO or AMO operators (Chapter 3) are normalized (Beasley and Mobley, 1988; Canning and Gardner, 1998; Chemingui, 1999). In more complex situations, in which the velocity in the overburden is sufficiently complex to distort the wavefield or even to cause illumination gaps, normalization should be applied in the image domain after full prestack migration (Bloor et al., 1999; Rickett, 2003).

Simple normalization of the imaging operators is not sufficient to remove imaging artifacts when illumination gaps are large. In such conditions, the data-modeling operator — which usually is defined as the adjoint of the imaging operator — should be inverted by a regularized inversion methodology. As is true for operator equalization, the methods proposed in the literature for inverting imaging operators can be divided into algorithms based on partial prestack migration (Ronen, 1987; Ronen and Liner, 2000; Chemingui and Biondi, 2002) and those based on full prestack migration. The methods use either a Kirchhoff

operator (Nemeth et al., 1999; Duquet et al., 2000) or a wavefield-continuation operator (Prucha and Biondi, 2002; Kuehl and Sacchi, 2002).

Iterative inversion is expensive, especially when a full prestack-migration operator is inverted. In this chapter, I present a noniterative method for regularizing the model space. It improves the quality of the reconstructed data without the computational cost of an iterative inversion. However, when there are large acquisition gaps or when the complexity of the overburden is responsible for incomplete illumination of the reflectors, expensive iterative regularized inversion is unavoidable. At the end of this chapter, we discuss some potential applications of iterative inversion.

Equalization of imaging operators

To explore the methods used to equalize imaging operators, I employ interpolation followed by partial stacking as a proxy of more complex imaging operators. As a proxy, interpolation has the advantage of being simple, easy to understand, and easy to manipulate analytically. Its analysis will lead us to discuss fundamental issues regarding spatial interpolation of seismic traces and normalization, or equalization, of imaging operators. The lessons we learn by using interpolation are applicable to the equalization of several imaging operators.

Stacking is the operation of averaging seismic traces by summation. It is an effective way to reduce the size of data sets and to enhance reflections while attenuating noise. To avoid attenuating the signal along with the noise, the reflections need to be coherent among the traces that are being stacked. To increase trace coherency, we can apply simple normal moveout (NMO) before stacking, or a partial-prestack-migration operator such as DMO or AMO (Chapter 3).

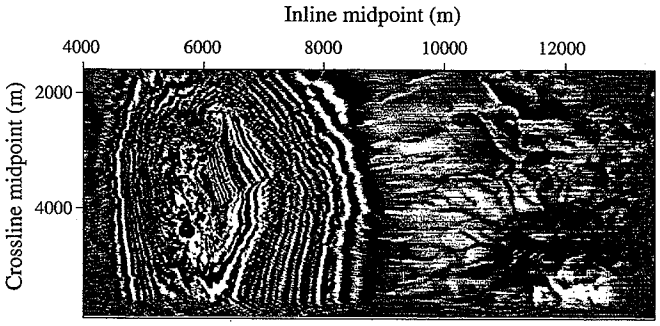

Figure 1. Example of acquisition footprint in a migrated depth slice. The horizontal stripes are related to the acquisition sail lines. Notice that the stripes bend when the reflectors start to dip in the vicinity of the salt ($x_m \approx 5500$ m).

Global stacking of all the traces recorded at the same midpoint location, regardless of their offset and azimuth, is the most common type of stacking. Partial stacking averages only those traces with their offset and azimuth within a given range. Partial stacking is useful if we want to preserve differences among traces when those differences are functions of the trace offset and azimuth and thus we must avoid global averaging. AVO studies are a useful application of partial stacking. Partial stacking also is useful when simple transformations, such as NMO, are not sufficient to correct for the differences in time delays among traces with very different offsets and azimuths. Such a situation is common when velocity variations cause nonhyperbolic moveouts in the data. Because data redundancy is low in partial stacking, the results of partial stacking are more likely to be affected by artifacts related to irregular acquisition geometries than are the results of global stacking. Thus, in this section, I will focus my analysis on partial stacking, but the methods I present here obviously can be applied to global stacking operators too.

To start our analysis, I define a simple linear model that links the recorded traces (at arbitrary midpoint locations) to the stacked volume (defined on a regular grid). Each data trace is the result of interpolating the stacked traces and is equal to the weighted sum of the neighboring stacked traces. The interpolation weights are functions of the distance between the midpoint location of the model trace and the midpoint location of the data trace. The sum of all the weights corresponding to one data trace usually is equal to one. Because the weights are independent of time along the seismic traces, for notational simplicity, we collapse the time axis and consider each element d_i of the data space (recorded data) $\mathbf{d}$ and each element m_j of the model space $\mathbf{m}$ (stacked volume) as representing a whole trace. The relationship between data and model is linear and can be expressed as

$$d_i = \Sigma_j \, l_{ij} \, m_j, \text{ subject to the constraint } \Sigma_j \, l_{ij} = 1. \quad (9.1)$$

In matrix notation, equation 9.1 becomes

$$\mathbf{d} = \mathbf{L}\mathbf{m}. \quad (9.2)$$

The simplest and crudest spatial interpolation is a nearest-neighborhood interpolation. For example, if we have three model traces and four data traces and we use a simple nearest-neighborhood interpolator, equation 9.2 becomes